BRAIN CONNECTIVITY
Volume 6, Number 10, 2016

DOI: 10.1089/brain.2016.0436

Human Posterior Insula Functional Connectivity Differs Between Electrical Pain and the Resting State

Keith M. Vogt,[1] Christopher J. Becker,[2] Ajay D. Wasan,[1,2] and James W. Ibinson[1,2]

Abstract

The objective in this study was to directly compare MRI-based functional connectivity between conditions of rest and painful electrical nerve stimulation for key regions involved in pain processing: the anterior and posterior insula and the anterior cingulate cortex. Electric nerve stimulation, rated 7/10 for pain, was delivered to the right index finger of 14 healthy pain-free adult volunteers in four 30-sec blocks and continuously for 2 min. Functional connectivity maps obtained at rest and during both pain tasks were compared using seed time courses from the left anterior and posterior insula and anterior cingulate. Significant Pain versus Rest connectivity differences were consistently shown for the posterior insula, notably to the posterior cingulate and precuneus, while minimal and inconsistent differences were observed for the anterior insula and anterior cingulate. This study reinforces the known differences that can occur with changes in seed region selection in functional connectivity analysis. It also presents preliminary evidence that functional connectivity for the left posterior insula can potentially differentiate the presence of acute right-sided electrical pain from the nonpainful resting state.

Keywords: blood oxygen level dependent signal; default mode network; electric nerve stimulation; functional connectivity MRI; insula; pain; posterior cingulate cortex

Introduction

Functional connectivity magnetic resonance imaging (fcMRI) has emerged as a technique to study interrelationships between brain regions. Low-frequency (<0.1 Hz) fluctuations in the blood oxygen level-dependent (BOLD) signal are systematically explored for temporal correlations between distant brain areas as these slow BOLD signal changes reflect regional blood flow oscillations (Liang et al., 2013) and are generally accepted to reflect meaningful periodic changes in underlying neuronal activity (Keilholz, 2014). These occur in an organized and coherent manner across brain areas that are functionally related, reflecting spontaneous neuronal activity, and are present at rest (Fox and Raichle, 2007).

Using both traditional functional MRI and advanced fcMRI analyses, studies have shown that pain processing involves several brain areas. These regions are activated by a range of salient stimuli (Legrain et al., 2011) and are typically divided into sensory processing components that include the primary (SI) and secondary (SII) somatosensory cortices and affective processing components focusing on the anterior cingulate cortex (ACC), amygdala, and medial prefrontal cortices (PFCs) (Brooks and Tracey, 2005; Peyron et al., 2000). However, we lack a complete understanding of the changes in functional connectivity that may occur during the experience of pain, including connections involving brain areas not classically known to be involved in pain processing (Kim et al., 2015; Kucyi and Davis, 2015).

The insula can be divided into distinct subdivisions, each with different resting-state functional connectivity (Taylor et al., 2009). This differential insular connectivity suggests that each portion may be responsible for different aspects of pain processing (Wiech et al., 2014). Peltz and colleagues previously demonstrated that the anterior insula (aIns) was more correlated with the ACC and PFC during noxious and non-noxious thermal stimulation. Meanwhile, the posterior insula (pIns) was more correlated with the primary sensory and motor cortices (Peltz et al., 2011), suggesting a sensory role, consistent with the known somatotopic organization of the pIns (Brooks et al., 2005). Further illustrating the importance of insula subdivision in the experience of pain, Kim et al. (2013) found that greater pIns to SI connectivity during experimental back pain in healthy subjects was associated with the need for a lower level of stimulus to reach the same subjective pain level.

The insula has been shown to have higher baseline connectivity to an organized set of areas known as the default mode network (DMN) in patients with various types of chronic low back pain (Kornelsen et al., 2013; Loggia

[1]Department of Anesthesiology, School of Medicine, University of Pittsburgh, Pittsburgh, Pennsylvania.
[2]Department of Anesthesiology, Center for Pain Research, University of Pittsburgh, Pittsburgh, Pennsylvania.

et al., 2013). A recent study in healthy subjects has also shown that experimental pain reduces the functional connectivity between the posterior insula and the posterior cingulate cortex (PCC), a component of the DMN (Zhang et al., 2014). DMN connectivity is seen when the subject is not attending to a task, and thus DMN activity probably reflects either an intrinsic resting brain state or attention to internal stimuli (Buckner et al., 2008). Thus, connectivity changes between the insula and the DMN may signal a shift in attention related to the experience of pain. Furthermore, our recent work examining the effect of global signal regression on functional connectivity maps of pain (Ibinson et al., 2015) suggested that the PCC and insula were differentially linked during pain and rest, but we did not examine the anterior and posterior insula separately.

The study presented here directly investigates MRI-based functional connectivity of the anterior and posterior subdivisions of the insula during painful electric nerve stimulation (ENS). Our primary hypothesis was that aIns to ACC functional connectivity would increase during pain processing compared with rest. We also compared the functional connectivity of the pIns to the ACC between pain and rest, expecting to find no differences. Furthermore, we expand on the prior work of other researchers by examining the interplay between the insula and the PCC and precuneus (PCun), which are core components of the DMN (Leech et al., 2012; Utevsky et al., 2014). The effect of longer stimulus duration is examined, and comparison with a no stimulation control is employed, rather than an innocuous level of sensory stimulation.

Methods

Subjects

This study was approved by the University of Pittsburgh institutional review board and complies with all relevant recommendations for responsible research. Subjects were screened for any contraindications to MRI as well as exclusion criteria, including current pregnancy or prescription medication use, history of current acute or chronic pain, history of psychiatric disorders (including depression and anxiety), and history of illicit substance use. Data are presented from 14 healthy right-handed subjects (11 males) with age ranging from 18 to 50 years.

Painful stimulation

ENS was used as the experimental stimulus. Just before entering the MRI environment, electrodes were placed on the lateral aspect of the subject's right index finger straddling the proximal interphalangeal joint. The nerve stimulator (EzStim II; Life Tech, Stafford, TX) gave a 100 Hz stimulation waveform (tetany setting) and the current flow was individualized for each subject to a subjective pain intensity rating of 7/10, with mean ± standard deviation of 19 ± 12 mA. The numerical pain scale was explained to subjects as ranging from 0 to 10, with anchors of 0 being no pain and 10 being highest pain imaginable. Once adjusted, this current level was used continuously throughout all pain stimulation periods as described below; amplitude and frequency of the stimulation waveform were not varied. Pain scores were not collected during scanning. However, in subjects undergoing this same paradigm, we have previously demonstrated that the electric shocks remain consistently painful throughout the experiment, including at the end (Ibinson and Vogt, 2013).

There were two ENS stimulation periods, the order of which was not varied, with imaging occurring continuously throughout the experiment, including the time between stimulation periods. Scanning began with a 3.5-min Rest scan, in which the subjects were asked to lie still with their eyes open. The first stimulation paradigm, referred to as Cyclic Pain, involved alternating between 30-sec periods of painful ENS and 30-sec periods of no stimulation in the block design ON/OFF pattern typical of task-based BOLD functional magnetic resonance imaging (FMRI) experiments. Four 30-sec pain periods were included for a total experiment time of 4.5 min. Subjects then experienced a 4-min period of no stimulation, thus avoiding any interference with subsequent stimulation (Ibinson et al., 2004), and data collected during this time were not analyzed as part of this study. A second period of 2 min of continuous painful stimulation then followed and these data are referred to as Tonic Pain.

Image data acquisition

Imaging was performed using a Siemens 3 Tesla Scanner (Siemens Medical Solutions, Malvern, PA). The FMRI data were acquired with a BOLD-weighted gradient echo sequence with the following parameters: TR 2 sec, TE 30 ms, flip angle 90°, matrix 64 × 64, in-plane resolution 3.125 × 3.125 mm, and slice thickness 4 mm. Thirty-five contiguous axial slices were collected in an interleaved manner, with whole brain coverage. Additionally, a high-resolution T1-weighted image (MPRAGE, with the following parameters: TR 25 sec, TE 5 ms, flip angle 35 degrees, matrix size 256 × 192, field of view 20 cm, in-plane resolution 1.2 mm, and slice thickness 2.8 mm) was acquired for all subjects for subsequent use in registration.

FMRI data processing

FMRI data sets were preprocessed using FSL (www.fmrib.ox.ac.uk/fsl) version 4.1.8; the following acronyms refer to subroutines within FSL unless otherwise specified, and the reader is referred to the FSL website for detailed explanations of these. FEAT version 5.98 was used, with brain extraction using BET (Smith, 2002) and motion correction with MCFLIRT (Jenkinson et al., 2002). The rotational and translational motion reports from registration in MCFLIRT were examined for excessive motion, and any MRI data with greater than 1.5 mm translation or more than two degrees of rotation were removed from further analysis as these criteria represent movement of more than half of the signal from a voxel being displaced from its expected location. One acquired dataset was discarded due to excessive detected motion. All reported results include only the 14 subjects that did not have significant head motion detected using the above algorithm and exclusion criteria. Spatial smoothing was performed with a Gaussian kernel of full width at half maximum of 6 mm. A Gaussian low-pass filter with a sigma of 2.8 sec was applied.

Functional connectivity analysis

The individual 4D datasets were then analyzed for functional connectivity. Three seed regions of interest (ROIs) were selected as areas to investigate. The majority of the

left insula (contralateral to the pain stimulus) and Brodmann area (BA) 24 of the ACC had previously been identified as strongly activated in a task-based analysis of the cyclic pain data (Ibinson and Vogt, 2013). We note that this area of the cingulate gyrus is what others have called the midcingulate cortex (Vogt, 2005), but to maintain consistency with our previous work, we subsequently refer to this region as ACC24. For this connectivity analysis, the local maximum voxels from the group average Cyclic Pain task activation, identified in our prior publication (Ibinson and Vogt, 2013), were used for the anterior and posterior portions of the left insula and the ACC24. These identified seed voxels had center coordinates (x, y, and z in mm) in the reference space of the Montreal Neurological Institute (MNI) standard space brain as follows: −36, 14, 4 for the anterior insula; −38, −4, 10 for the posterior insula; and −2, −12, 44 for ACC24).

Around each identified seed voxel, a 6 mm radius sphere was then generated. These small spherical ROI masks are shown in Figure 1. Each ROI was transformed into the lower resolution coordinate space of the individual subject's functional images using the registration matrices from FLIRT and the average signal intensity time courses were extracted from each 4D dataset using the Featquery subroutine of FSL. These average ROI time courses were then used as the main explanatory variables in the FSL regression analyses to determine functional connectivity to other brain areas. FILM prewhitening was applied. For each dataset, the time courses of image motion from MCFLIRT and the whole-brain mean MR signal time course were regressed as effects of no interest. These measures minimize the impact of residual motion occurring on a subvoxel scale and any effects from signal drift during the scan run, respectively, as recommended by our own experience (Ibinson et al., 2015) and an fcMRI analysis review (Van Dijk et al., 2010). For the Cyclic Pain task, the stimulation paradigm timing was also included as a regressor of no interest based on our previous optimization recommending inclusion (Ibinson et al., 2015).

Group map generation

For group analysis, individual subject's BOLD functional images were registered first to their high-resolution structural image and then to the MNI standard space brain using FLIRT. Maps of group average connectivity were generated using a mixed-effects analysis using FLAME (two stage). Significant connectivity clusters are displayed with a threshold of $Z > 2.3$ with a cluster-corrected significance of $P = 0.05$. Connectivity maps were rendered for publication using MRIcro version 1.4 (www.mricro.com). All images are displayed in radiologic convention and a preset color scale with Z-score range as shown in each figure. Positive correlations are shown in warm colors, as is typical in the literature. We have previously demonstrated the importance of accounting for anticorrelations in analyses that include global signal regression (Ibinson and Vogt, 2014). Thus, inverse correlation maps were calculated and, when present, are concurrently displayed in the average connectivity maps using cool colors. Pain versus Rest and Tonic Pain versus Cyclic Pain difference maps were also computed using a mixed-effects model and rendered similar to the average connectivity maps. For these figures, the warm color overlay displays the magnitude of greater pain connectivity, compared with rest; the cool colors show rest greater than pain connectivity differences. To directly compare for Pain versus Rest connectivity differences between the anterior versus posterior insula, a 2-level contrast was performed on the datasets, which can be described as follows: (aIns_Pain − aIns_Rest) − (pIns_Pain − pIns_Rest). Because of the many possible directions of effect in this two-level contrast, an F-test was used to indicate significant areas of difference, without showing the directionality.

Results

Seed region connectivity by experimental condition

Connectivity results using the seed time course from the anterior portion of the left insular cortex (contralateral to the pain stimulus) are shown in Figure 2. Each row in the figure displays one of the three different datasets, Rest, Cyclic Pain, and Tonic Pain. The selected slices (for all figures) shown left to right are numbers 65, 55, 45, and 24 from the MNI standard brain. Common areas of correlation with the left anterior insula across all three task periods are limited to the ACC and right insula. The Cyclic Pain and Rest data show correlations with the bilateral secondary somatosensory cortices. The Cyclic Pain dataset showed some anticorrelation with the PCC and PCun (which will be referred to as PCC/PCun) and portions of the cerebellum.

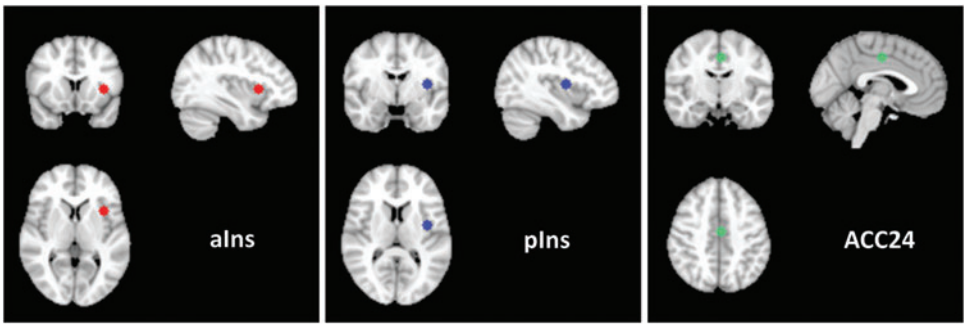

FIG. 1. Anatomic locations of the seed regions used for functional connectivity magnetic resonance imaging analysis shown on the Montreal Neurological Institute standard brain. The anterior portion of the left insula is shown in red in the left panel (center coordinates = −36, 14, 4). The posterior portion of the left insula is shown in blue in the center panel (center coordinates = −38, −4, 10). The anterior cingulate cortex seed from BA24 (ACC24) is shown in green in the right panel (center coordinates = −2, −12, 44). aIns, anterior insula; pIns, posterior insula. Color images available online at www.liebertpub.com/brain

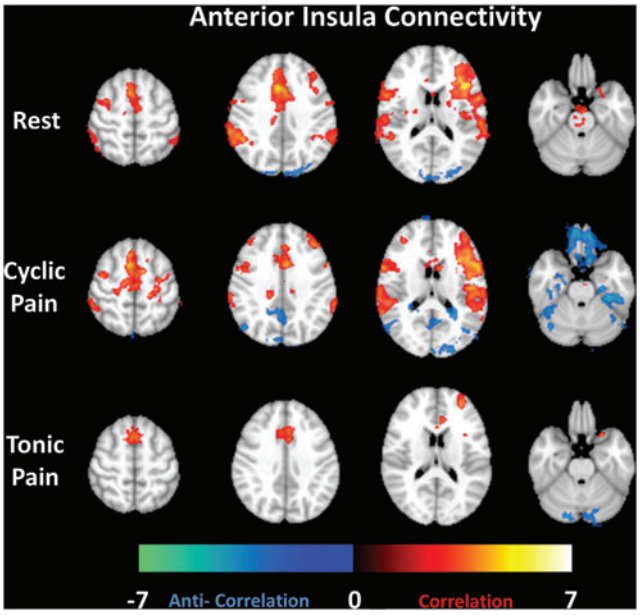

FIG. 2. Group average connectivity maps (selected slices) for a seed region in the anterior insula for the Rest, Cyclic Pain, and Tonic Pain datasets (by row). Z-scores representing the strength of correlation (warm colors) or anticorrelation (cool colors) are shown by the color bar at the bottom. Color images available online at www.liebertpub.com/brain

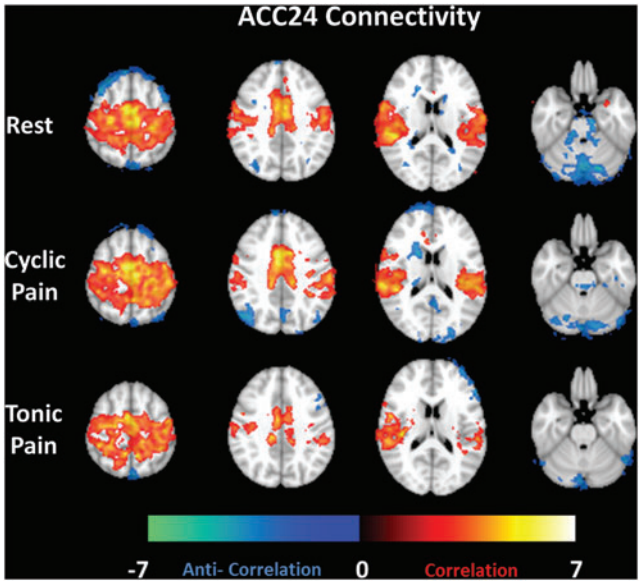

FIG. 4. Group average connectivity maps (selected slices) for a seed region in the anterior cingulate cortex (BA24) for the Rest, Cyclic Pain, and Tonic Pain datasets (by row). Z-scores representing the strength of correlation (warm colors) or anticorrelation (cool colors) are shown by the color bar at the bottom. Color images available online at www.liebertpub.com/brain

Similarly, connectivity using the posterior portion of the left insula as the seed region is displayed in Figure 3. Notable areas of correlation across all datasets include the right insula, bilateral primary and secondary somatosensory cortices, and the ACC. Portions of the PCC/PCun are anticorrelated with the posterior insula. Anticorrelation in different portions of the PFC is also evident in all datasets.

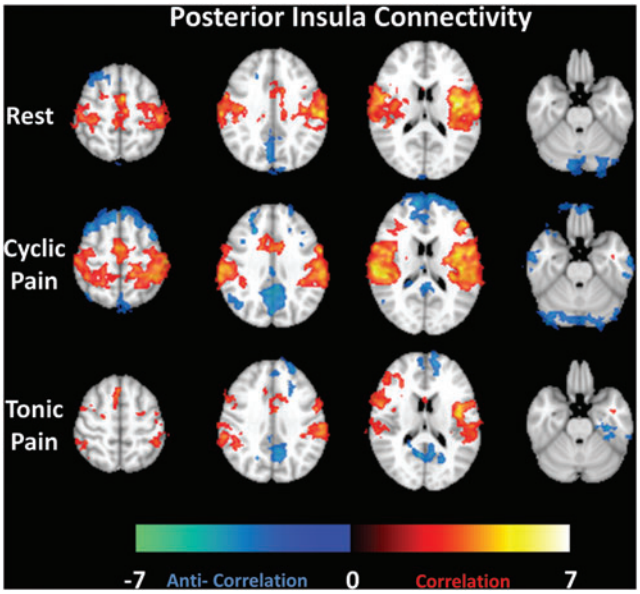

FIG. 3. Group average connectivity maps (selected slices) for a seed region in the posterior insula for the Rest, Cyclic Pain, and Tonic Pain datasets (by row). Z-scores representing the strength of correlation (warm colors) or anticorrelation (cool colors) are shown by the color bar at the bottom. Color images available online at www.liebertpub.com/brain

When the fcMRI seed region is taken from the ACC24 (Fig. 4), the connectivity maps show reciprocal connectivity to the bilateral insular cortices. Anticorrelation is seen with a small area of the PCC/PCun in the Cyclic Pain data. This is consistent with the relationship shown for this brain structure with left insular seed analyses. Anticorrelation is also seen with portions of the cerebellum, particularly in the Rest data.

Table 1 summarizes the strength of connectivity, indicated by the local maximum Z-score for the analyses with the three seed regions described. As a point of clarification, the connectivity clusters in Table 1, which are given anatomical labels, do not necessarily encompass (and certainly do not entirely comprise) the voxels used to calculate the seed time courses with the same or similar names. The ROIs that are quantified here include those with consistent involvement in processing acute pain (Apkarian et al., 2005; Duerden and Albanese, 2013; Peyron et al., 2000). The strongest overall correlation is seen from the left insula (either anterior or posterior subdivisions) to the right insula. Mixed-effects contrasts between the Tonic and Cyclic pain datasets for both the aIns and pIns were calculated, but found to lack significant clusters of connectivity (blank maps not shown).

Pain versus Rest functional connectivity differences

Difference maps are shown in Figure 5 for Cyclic Pain versus Rest and in Figure 6 for Tonic Pain versus Rest. The same brain slices as in Figures 2–4 are shown; each row displays maps from different seed regions. Both pain datasets have commonalities in their difference maps compared with the Rest dataset. There are minimal Cyclic or

Table 1. Functional Connectivity Cluster Details

	Rest		*Cyclic Pain*		*Tonic Pain*	
Brain region	*Z-Max*	*x, y, z*	*Z-Max*	*x, y, z*	*Z-Max*	*x, y, z*
aIns Seed						
Right Insula	6.15	34, 20, 0	5.11	34, 20, 2	4.27	48, 6, −2
ACC (BA 24)	4.60	2, 18, 40	3.44	−2, 12, 42	3.98	0, 20, 20
Left SI	—	—	2.54	−34, −32, 62	—	—
Left SII	3.45	−62, −32, 18	3.92	−60, −26, 22	—	—
BA 17 (L Cuneus)	−3.74	−32, −88, 10	−2.94	−24, −96, 14	—	—
BA 17 (R Cuneus)	—	—	—	—	—	—
sgACC	—	—	−4.34	−10, 32, −14	—	—
Right SII	3.01	60, −20, 16	3.55	68, −28, 12	—	—
BA 6	—	—	—	—	3.46	4, 16, 56
Left Crus I	—	—	—	—	−3.01	−14, −82, −30
BA 9	—	—	—	—	4.37	−28, 50, 22
Precuneus	—	—	−3.94	−4, −62, 24	—	—
PCC	—	—	−3.44	6, −50, 34	—	—
pIns Seed						
Right Insula	4.02	40, −4, 4	5.00	36, 2, 10	3.38	34, 0, 8
ACC (BA 24)	3.03	−6, 8, 40	4.13	8, 20, 42	3.65	0, 8, 30
Left SI	3.87	−48, −34, 48	4.88	−60, −28, 42	3.87	−44, −32, 40
Left SII	5.19	−62, −10, 22	4.54	−66, −26, 24	3.38	−58, −32, 20
Right SI	3.35	36, −30, 54	4.34	56, −20, 52	3.65	62, −36, 38
Right SII	4.45	52, −10, 26	5.86	62, −26, 18	4.05	48, −26, 10
Lingual Gyrus	−3.75	−30, −56, −2	—	—	—	—
BA 8/BA 6	−3.10	26, 28, 50	−4.3	26, 26, 46	—	—
Left Crus I	−4.04	−24, −70, −34	—	—	—	—
Precuneus	−3.89	8, −68, 32	−3.72	4, −64, 32	−3.79	−6, −60, 32
PCC	−2.72	4, −40, 28	−4.40	4, −48, 32	−3.97	10, −50, 24
ACC Seed						
Left Insula	4.69	−46, −26, 6	4.68	−38, 6, −2	—	—
Right SII	5.82	52, −36, 20	5.52	60, −26, 20	4.91	58, −34, 20
Vermis	−5.23	0, −44, −38	−3.44	6, −40, −38	—	—
Left SII	4.18	−64, −8, 14	4.39	−48, −32, 10	4.30	−58, −32, 18
R Cuneus	−3.23	32, −76, 40	−4.34	44, −66, 30	—	—
L Cuneus	−3.11	−34, −80, 30	−3.05	−50, −72, 30	—	—
Precuneus	—	—	−3.13	−4, −72, 32	—	—
PCC	—	—	−2.99	−2, −52, 18	—	—
Right Insula	4.51	62, −10, 2	4.96	38, 0, 6	3.64	44, 2, 6

Local maximum Z-score (Max Z) and corresponding coordinates in the MNI standard space brain for connectivity clusters in the Rest, Cyclic Pain, and Tonic Pain datasets analyzed with seed regions in the left anterior and posterior insular cortices and the ACC24. Negative Z-scores reflect anticorrelation (further explained in the text). sgACC refers to the subgenual portion of the ACC in BA 32.

ACC, anterior cingulate cortex; aIns, anterior insula; BA, Brodmann area; MNI, Montreal Neurological Institute; PCC, posterior cingulate cortex; pIns, posterior insula; SI, primary somatosensory cortex; SII, secondary somatosensory cortex.

Tonic Pain versus Rest connectivity differences for the aIns and ACC24 seed regions (first and third rows). Connectivity differences from the pIns seed region (second rows in Figs. 5 and 6) include areas activated in task-based studies of pain. Table 2 lists the differences for the Cyclic/Tonic Pain versus Rest contrasts for each seed region. Specifically, pIns connectivity to the PCC, lingual gyrus, supplementary motor area, and cerebellum in both the Cyclic and Tonic Pain data was significantly greater than in the Rest data (greater in this case meaning that the values were closer to zero). Rest greater than pain connectivity was seen in the Tonic Pain data (second row of Figs. 5 and 6) in the ACC, left primary and bilateral secondary somatosensory cortices, and right insula. The comparatively fewer clusters showing significant Cyclic/Tonic Pain versus Rest differences for the aIns and ACC24 are also listed in Table 2.

Anterior versus posterior insula functional connectivity differences

Figure 7 shows the areas where the Pain versus Rest connectivity differences are significantly different between the anterior versus posterior insula. This F-test map does not indicate the directionality of greater versus lesser connectivity, and it would be difficult to show all possible combinations on one map. However, significant differences shown in Figure 7 reflect the differences seen visually in the single-level Pain versus Rest contrast maps of Figures 5 and 6.

Discussion

This study compared fcMRI maps in healthy subjects while at rest and during the experience of acute electrical pain stimulation of two durations. We demonstrate that

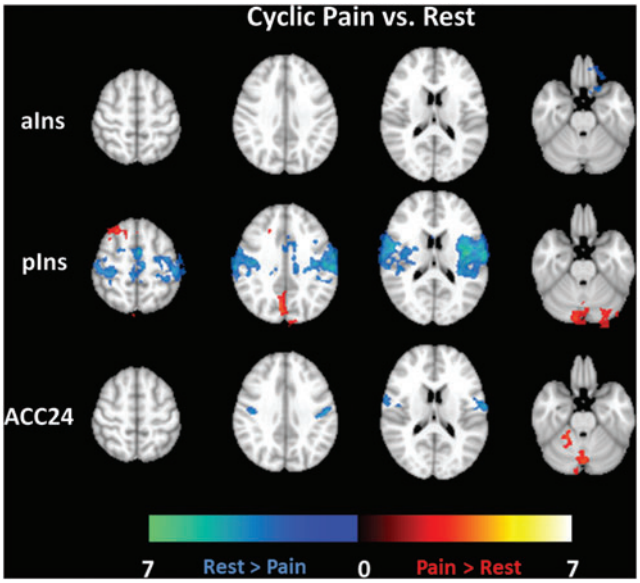

FIG. 5. Contrast maps for Cyclic Pain versus Rest connectivity differences for each seed region analysis (rows). The color bars define the range of Z-score differences shown. Warm colors indicate a Pain > Rest difference, while cool colors show areas where Rest > Pain. Color images available online at www.liebertpub.com/brain

fcMRI maps can be obtained during task performance, even if the tasks differ in paradigm timing pattern or length. It should be noted that the results we display for cyclic pain include regression of the task paradigm, previously demonstrated to focus the analysis on low-frequency neuronal-generated signals. A seed region analysis for the insula and ACC was used for several reasons: these areas are known to be fundamentally involved in pain processing (Duerden and Albanese, 2013), they demonstrate resting-state connectivity to each other (van den Heuvel and Hulshoff Pol, 2010), they demonstrate differences in fcMRI during painful experimental tasks (Peltz et al., 2011; Zhang et al., 2014), and both areas show interconnectivity changes in chronic pain patients (Ichesco et al., 2012).

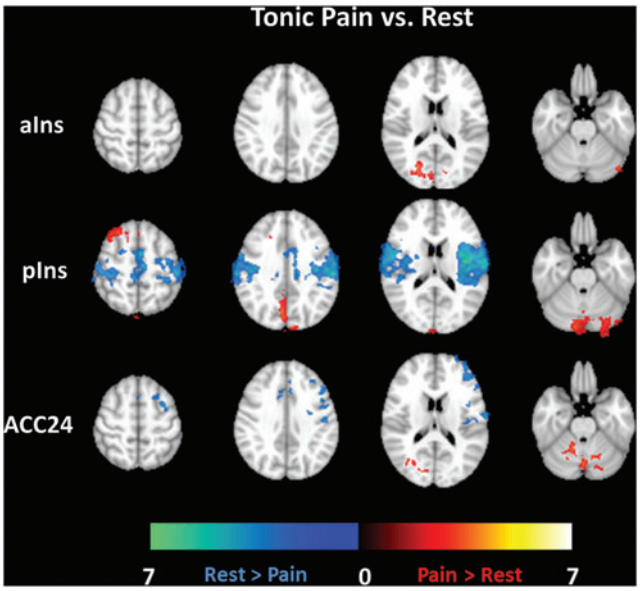

FIG. 6. Contrast maps for Tonic Pain versus Rest connectivity differences for each seed region analysis (rows). The color bars define the range of differences shown, as described previously. Color images available online at www.liebertpub.com/brain

Based on pain-related functional connectivity differences demonstrated in prior work, we separately explored the anterior and posterior subdivisions of the insula. Figures 2 and 3 show that the connectivity of the two left insular seed regions demonstrated the expected connectivity (Peltz et al., 2011). However, Figures 5 and 6 clearly show greater Pain versus Rest differences for the pIns connectivity maps for both the Cyclic (30 sec) and Tonic (2 min) pain stimulation paradigms and Figure 7 demonstrates that these differences are significant. Meanwhile, the aIns and ACC seed ROIs showed minimal and inconsistent significant differences between Pain and Rest. The most notable feature of the connectivity difference maps is the concordance between the Cyclic and Tonic pain datasets for pIns connectivity to the PCC/PCun (as representative regions of the DMN) and left cerebellum. In large part, these pIns differences seem to be driven by the anticorrelations in the Rest maps (cool colors in top row of Fig. 3) that are reduced or absent in the Cyclic or Tonic Pain maps. The lack of differences in these areas for the aIns seems to be due to the persistence of these anticorrelations during Pain.

Correlation between insular connectivity and successful treatment of chronic low back pain has been shown (Ceko et al., 2015). This is partly the rationale for our choosing a rest control, instead of a nonpainful level of electrical stimulation, which is typically experienced as tingling (Ibinson et al., 2004). We acknowledge that comparison with a nonpainful sensory stimulation state would allow more specificity for pain and would be more similar to other previous work (Peltz et al., 2011). However, the nonpainful state in clinical patients is not typically one in which they experience nonpainful somatosensory stimulation in the area of concern. Thus, tracking the successful treatment of a chronic pain syndrome would be more like having patients experience a resting state. As a result, our experimental design sets up an fcMRI analysis that is more likely to detect the presence of intense stimulation, including pain, at the expense of being less specific to the pain experience apart from the noxious somatosensory stimulation that is causing it.

However, counter to our original hypothesis, we did not demonstrate a consistent relationship for insula to ACC connectivity during our two pain tasks. Our results did not reproduce the differential fcMRI for the insular subregions between Pain and Rest that was previously shown between painful and nonpainful thermal stimuli (Peltz et al., 2011). Specifically, Peltz et al. found greater aIns to ACC connectivity during pain, while we showed a slight increase in connectivity during cyclic pain and a considerable decrease during the Tonic Pain task. This could relate to differences in task length or task type, as Zhang et al. (2014) found that a painful injection of hypertonic saline (arguably more similar to our Tonic Pain task) decreased ACC to aIns connectivity. Although it is the reciprocal direction, our aIns data support this, showing a decrease in connectivity strength for both Cyclic and Tonic Pain compared with Rest (Table 1 and Fig. 2). Pain and Rest comparison results for the pIns show the opposite relationship: an increase in pIns to ACC connectivity is seen for both pain

Table 2. Functional Connectivity Cluster Details for the Pain—Rest Comparison

	Cyclic Pain vs. Rest		*Tonic Pain vs. Rest*	
Brain region	*Z-Max*	*x, y, z*	*Z-Max*	*x, y, z*
aIns Seed				
sgACC	−4.05	−10, 34, −12	—	—
BA 17 (R Cuneus)	—	—	4.18	8.−84, 12
BA 17 (L Cuneus)	—	—	4.07	−32, −82, −4
pIns Seed				
Right Insula	−4.96	36, −6, 6	−5.12	36, −6, 6
ACC (BA24)	−4.92	−4, 0, 52	−5.09	−2, 0, 54
Left SI	−5.51	−60, −20, 42	−5.32	−60, −40, 40
Left SII	−5.52	−64, −16, 18	−5.59	−64, −16, 18
Right SII	−5.18	62, −4, 8	−5.13	62, −6, 10
Left Crus I	4.01	−24, −70, −34	3.72	−24, −70, −32
Precuneus	3.72	8, −68, 32	3.70	6, −70, 32
PCC	—	—	2.63	4, −44, 28
Lingual Gyrus	3.77	−30, −56, −2	3.66	−28, −72, −2
BA 8/BA 6 (SMA)	2.97	26, 28, 50	3.33	28, 28, 52
ACC Seed				
Left SI	−3.84	−50, −18, 38	−3.40	−48, −16, 38
Right SI	−3.49	42, −16, 32	—	—
Vermis	3.28	−2, −74, −26	3.58	−4, −64, −18
BA 9	—	—	−4.445	−46, 26, 32
BA 6	—	—	−3.32	0, 6, 66

Local maximum Z-score (Max Z) and corresponding coordinates in the MNI standard space brain for connectivity clusters in the Cyclic Pain versus Rest and Tonic Pain versus Rest datasets. Z-scores are given for seed regions in the left anterior and posterior insular cortices. Negative values reflect Rest > Pain scores, while positive Z-scores are given if Pain > Rest. sgACC refers to the subgenual portion of the ACC in BA 32.

datasets, compared with Rest (Table 1 and Fig. 3). This is also consistent with the work of Zhang et al. (2014). Our pIns results differ from Peltz's study (Peltz et al., 2011); we did not demonstrate an fcMRI difference between the pIns (or any ROI examined) and SI or MI. Our use of Rest, without a somatosensory task, for comparison with Pain actually favors our study being likely to detect differences in these somatosensory discrimination areas. It is possible that differences in stimulus modality (thermal versus electrical pain), stimulus duration, or fcMRI analysis techniques may explain these conflicting results.

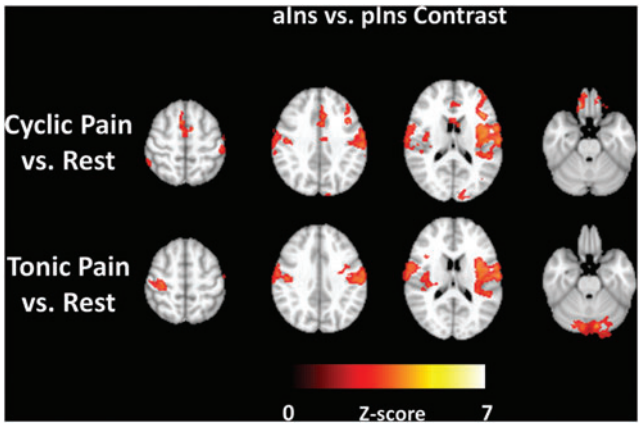

FIG. 7. Selected slices from the group-level contrast between the aIns and pIns comparing connectivity difference maps between Cyclic Pain and Rest (top row) and between Tonic Pain and Rest (bottom row). Z-scores shown by the color bar represent the significance of connectivity differences calculated with an F-test. Color images available online at www.liebertpub.com/brain

There has been increasing interest in recent years in the role of the DMN in many cognitive functions, including pain processing. Thus, the significant Cyclic and Tonic Pain versus Rest pIns connectivity differences involving the PCC and PCun are not unexpected as these are both prominent components of the DMN (Leech et al., 2012; Utevsky et al., 2014). We found that the resting-state connectivity to the PCC/PCun was negative (anticorrelation) for the pIns, with no significant relationship found for the aIns. This compares favorably with the finding by Loggia et al. (2013) that DMN connectivity to the insula is altered by induced pain as their mid-insula connectivity cluster closely approximates our posterior insula ROI (coordinates listed in Table 3). It should be noted that our resting (baseline) insula to PCC/PCun connectivity was negative, while theirs was positive. This is likely due to the use of global signal regression, a key difference in our methods; however, we believe that the more important point is that a similar area of the insula was identified in both studies.

As alluded to above, there are notable differences in insula seed region definition reported in the literature. Table 3 lists the coordinates of some of the different insula seed regions or connectivity clusters reported in previous articles. There seems to be no consensus of what names should be applied to which regions of the insula. Furthermore, it is possible that parcellation of the insula into even smaller subregion seeds, such as those identified by prior data-driven imaging work (Deen et al., 2011; Kelly et al., 2012), could change our results. Our seed regions would overlap several of

Table 3. Summary of Coordinates of Insular Subregions Defined by This and Previous Articles Using Functional Connectivity Magnetic Resonance Imaging

Study	ROI label	MNI coordinates		
		x	*y*	*z*
Current study	L Anterior Insula	−36	14	4
	L Posterior Insula	−38	−4	10
Ichesco et al. (2012)	R Anterior insula	32	16	6
	L Anterior insula	−32	16	6
	R Posterior Insula	39	−15	8
	L Posterior Insula	−39	−15	1
Taylor et al. (2009)[a]	R Anterior Insula	40	18	−4
	L Anterior Insula	−35	16	−3
	R Middle Insula	42	3	2
	L Middle Insula	−39	0	3
	R Posterior Insula	42	−9	4
	L Posterior Insula	−39	−11	5
Zhang et al. (2014)	R Anterior Insula	32	16	6
	L Anterior Insula	−32	16	6
	R Posterior Insula	39	−15	8
	L Posterior Insula	−39	−15	1
Kim et al. (2015)	R Anterior Insula	32	18	0
	R Middle Insula	40	2	−10
	R Posterior Insula	34	−14	24
Loggia et al. (2013)	R Middle Insula	44	−4	0
Deen et al. (2011)	R Ventral Anterior Insula	32	10	−6
	L Ventral Anterior Insula	−33	13	−7
	R Dorsal Anterior Insula	35	7	3
	L Dorsal Anterior Insula	−38	6	2
	R Posterior Insula	35	−11	6
	L Posterior Insula	−38	−6	5

[a]Coordinates converted from Talairach space coordinates.
ROI, region of interest.

these much smaller subregions of the insular cortex, but we were focused on major differences in connectivity between the insula and other brain structures, rather than trying to elucidate fine scale differences in functional anatomy within the insula. In addition to differences in seed region definitions, our findings may differ from previous work of other groups due to choices made in the fcMRI analysis, as mentioned above.

As with any scientific endeavor, the work presented herein is not without limitations. We sought to explore the effects of different lengths of painful ENS on fcMRI, compared with the resting state, for key ROIs known to have their connectivity modulated by the experience of pain. We did not seek to exhaustively explore all regions of the brain, nor vary the modality of painful simulation (in the same set of subjects), nor explore the effects that a pain task longer than 2 min would have on fcMRI. Furthermore, we did not vary the order of presentation of the rest and pain tasks. Although MRI signal drift should be eliminated by our data processing pipeline, cognitive fatigue or habituation could cloud comparisons between the Cyclic (presented first) and Tonic (presented second) Pain tasks. However, the focus of our work was not to draw conclusions about differences between these two tasks, but rather see how each compared with the nonpainful resting state. Finally, we did not obtain real-time pain scores from all subjects. However, the same pain experimental paradigm was performed outside the scanner by a subset of the same subjects, and the stimulus was consistently rated as painful for both the Cyclic and Tonic Pain. Thus, we have no reason to think that habituation is a significant confound.

Our results are consistent with elements of other groups' work, but we found differences that could perhaps be explained by comparing insular subregion fcMRI with additional pain stimulus modalities and/or datasets of longer duration. It is notable that fcMRI studies are typically performed with 6 min (or more) of continuous data (Van Dijk et al., 2010). However, the minimum time period for successful fcMRI data is not known and may depend on task length or uncontrolled shifts in attention away from the intended focus on task or rest. The similarity in our fcMRI results between the Cyclic Pain dataset (4.5 min) and the Tonic Pain data (2 min) suggests that there are no drastic differences in statistical power, despite differences in the number of data time points. The longer Cyclic Pain task contained a number of time points that would generally be considered adequate for fcMRI; we extend this to suggest that the lack of major differences between the Cyclic and Tonic Pain maps provides evidence that the Tonic Pain task is also adequately powered. This is further supported by greater strength of correlation determined for some brain regions in the Tonic Pain dataset, which is the shortest. The lack of a consistent connectivity coefficient trend (i.e., Tonic < Cyclic/Rest) when comparing Z-statistics between datasets (Table 1) argues against the idea that connectivity differences are simply due to a relative underpowering of the shorter datasets; however, this possibility should be mentioned as a limitation, and we recommend that future studies use consistent task lengths.

Conclusions

This study compared resting-state fcMRI with that during two task periods of different durations of right-sided acute painful ENS. We found notable pain versus rest differences for both pain tasks when a seed time course from the left posterior insula was used and changes in connectivity to the PCC/PCun were most notable. These Pain versus Rest connectivity differences between the anterior and posterior insula were statistically significant. Meanwhile, seed regions in the left anterior insula and ACC24 showed minimal differences between pain and rest. Counter to our expectation, significant pain versus rest differences in insula to ACC connectivity were not observed. We propose that fcMRI correlation between the posterior insula and the DMN may differentiate pain from the nonpainful resting state using fcMRI.

Acknowledgments

This research was made possible by an NIH Grant Number T32GM075770, a Department of Anesthesiology Seed Grant, Grant Number 5UL1 RR024153-04 from the National Center for Research Resources (NCRR, a component of the NIH), and NIH Roadmap for Medical Research. This work is solely the responsibility of the authors and does not necessarily represent the official view of NCRR or NIH.

Author Disclosure Statement

No competing financial interests exist.

References

Apkarian AV, Bushnell MC, Treede RD, Zubieta JK. 2005. Human brain mechanisms of pain perception and regulation in health and disease. Eur J Pain 9:463–484.

Brooks J, Tracey I. 2005. From nociception to pain perception: imaging the spinal and supraspinal pathways. J Anat 207:19–33.

Brooks JC, Zambreanu L, Godinez A, Craig AD, Tracey I. 2005. Somatotopic organisation of the human insula to painful heat studied with high resolution functional imaging. Neuroimage 27:201–209.

Buckner RL, Andrews-Hanna JR, Schacter DL. 2008. The brain's default network: anatomy, function, and relevance to disease. Ann N Y Acad Sci 1124:1–38.

Ceko M, Shir Y, Ouellet JA, Ware MA, Stone LS, Seminowicz DA. 2015. Partial recovery of abnormal insula and dorsolateral prefrontal connectivity to cognitive networks in chronic low back pain after treatment. Hum Brain Mapp 36:2075–2092.

Deen B, Pitskel NB, Pelphrey KA. 2011. Three systems of insular functional connectivity identified with cluster analysis. Cereb Cortex 21:1498–1506.

Duerden EG, Albanese MC. 2013. Localization of pain-related brain activation: a meta-analysis of neuroimaging data. Hum Brain Mapp 34:109–149.

Fox MD, Raichle ME. 2007. Spontaneous fluctuations in brain activity observed with functional magnetic resonance imaging. Nat Rev Neurosci 8:700–711.

Ibinson JW, Small RH, Algaze A, Roberts CJ, Clark DL, Schmalbrock P. 2004. Functional magnetic resonance imaging studies of pain: an investigation of signal decay during and across sessions. Anesthesiology 101:960–969.

Ibinson JW, Vogt KM. 2013. Pain does not follow the boxcar model: temporal dynamics of the BOLD fMRI Signal during constant current painful electric nerve stimulation. J Pain 14:1611–1619.

Ibinson JW, Vogt KM. 2014. Effect of anti-correlations on statistical comparisons between pain task and resting fcMRI datasets. J Pain 15:S58.

Ibinson JW, Vogt KM, Taylor KB, Dua SB, Becker CJ, Loggia M, et al. 2015. Optimizing and interpreting insular functional connectivity maps obtained during acute experimental pain: the effects of global signal and task paradigm regression. Brain Connect 5:649–657.

Ichesco E, Quintero A, Clauw DJ, Peltier S, Sundgren PM, Gerstner GE, et al. 2012. Altered functional connectivity between the insula and the cingulate cortex in patients with temporomandibular disorder: a pilot study. Headache 52:441–454.

Jenkinson M, Bannister P, Brady M, Smith S. 2002. Improved optimization for the robust and accurate linear registration and motion correction of brain images. Neuroimage 17:825–841.

Keilholz SD. 2014. The neural basis of time-varying resting-state functional connectivity. Brain Connect 4:769–779.

Kelly C, Toro R, Di Martino A, Cox CL, Bellec P, Castellanos FX, et al. 2012. A convergent functional architecture of the insula emerges across imaging modalities. Neuroimage 61:1129–1142.

Kim J, Loggia ML, Cahalan CM, Harris RE, Beissner F, Garcia RG, et al. 2015. The somatosensory link in fibromyalgia: functional connectivity of the primary somatosensory cortex is altered by sustained pain and is associated with clinical/autonomic dysfunction. Arthritis Rheumatol 67:1395–1405.

Kim J, Loggia ML, Edwards RR, Wasan AD, Gollub RL, Napadow V. 2013. Sustained deep-tissue pain alters functional brain connectivity. Pain 154:1343–1351.

Kornelsen J, Sboto-Frankenstein U, McIver T, Gervai P, Wacnik P, Berrington N, et al. 2013. Default mode network functional connectivity altered in failed back surgery syndrome. J Pain 14:483–491.

Kucyi A, Davis KD. 2015. The dynamic pain connectome. Trends Neurosci 38:86–95.

Leech R, Braga R, Sharp DJ. 2012. Echoes of the brain within the posterior cingulate cortex. J Neurosci 32:215–222.

Legrain V, Iannetti GD, Plaghki L, Mouraux A. 2011. The pain matrix reloaded: a salience detection system for the body. Prog Neurobiol 93:111–124.

Liang X, Zou Q, He Y, Yang Y. 2013. Coupling of functional connectivity and regional cerebral blood flow reveals a physiological basis for network hubs of the human brain. Proc Natl Acad Sci U S A 110:1929–1934.

Loggia ML, Kim J, Gollub RL, Vangel MG, Kirsch I, Kong J, et al. 2013. Default mode network connectivity encodes clinical pain: an arterial spin labeling study. Pain 154:24–33.

Peltz E, Seifert F, DeCol R, Dorfler A, Schwab S, Maihofner C. 2011. Functional connectivity of the human insular cortex during noxious and innocuous thermal stimulation. Neuroimage 54:1324–1335.

Peyron R, Laurent B, Garcia-Larrea L. 2000. Functional imaging of brain responses to pain. A review and meta-analysis. Neurophysiol Clin 30:263–288.

Smith SM. 2002. Fast robust automated brain extraction. Hum Brain Mapp 17:143–155.

Taylor KS, Seminowicz DA, Davis KD. 2009. Two systems of resting state connectivity between the insula and cingulate cortex. Hum Brain Mapp 30:2731–2745.

Utevsky AV, Smith DV, Huettel SA. 2014. Precuneus is a functional core of the default-mode network. J Neurosci 34:932–940.

van den Heuvel MP, Hulshoff Pol HE. 2010. Exploring the brain network: a review on resting-state fMRI functional connectivity. Eur Neuropsychopharmacol 20:519–534.

Van Dijk KR, Hedden T, Venkataraman A, Evans KC, Lazar SW, Buckner RL. 2010. Intrinsic functional connectivity as a tool for human connectomics: theory, properties, and optimization. J Neurophysiol 103:297–321.

Vogt BA. 2005. Pain and emotion interactions in subregions of the cingulate gyrus. Nat Rev Neurosci 6:533–544.

Wiech K, Jbabdi S, Lin CS, Andersson J, Tracey I. 2014. Differential structural and resting state connectivity between insular subdivisions and other pain-related brain regions. Pain 155: 2047–2055.

Zhang S, Wu W, Huang G, Liu Z, Guo S, Yang J, et al. 2014. Resting-state connectivity in the default mode network and insula during experimental low back pain. Neural Regen Res 9:135–142.

Address correspondence to:
James W. Ibinson
Department of Anesthesiology
Center for Pain Research
University of Pittsburgh
200 Lothrop Street
W1445 Biomedical Science Tower
Pittsburgh, PA 15213

E-mail: ibinsonjw@upmc.edu